



On the four-quark operator matrix elements for the lifetime of Λ_b

Zhen-Xing Zhao^{1,a}, Xiao-Yu Sun¹, Fu-Wei Zhang¹, Zhi-Peng Xing^{2,b}

¹ School of Physical Science and Technology, Inner Mongolia University, Hohhot 010021, China

² Tsung-Dao Lee Institute, Shanghai Jiao Tong University, Shanghai 200240, China

Received: 8 August 2023 / Accepted: 27 November 2023 / Published online: 18 January 2024
© The Author(s) 2024

Abstract Heavy quark expansion can nicely explain the lifetime of Λ_b . However, there still exist sizable uncertainties from the four-quark operator matrix elements of Λ_b in $1/m_b^3$ corrections, which describe the spectator effects. In this work, these four-quark operator matrix elements are investigated using full QCD sum rules for the first time. At the QCD level, contributions from up to dimension-6 four-quark operators are considered. Our method for calculating high-dimensional operator matrix elements holds promise for use in resolving the Ω_c lifetime puzzle.

1 Introduction

In 2018, the Large Hadron Collider beauty (LHCb) experiment measured the lifetime of Ω_c^0 using $\Omega_b^- \rightarrow \Omega_c^0 \mu^- \bar{\nu}_\mu X$ decays and obtained [1]

$$\tau(\Omega_c^0) = 268 \pm 24 \pm 10 \pm 2 \text{ fs}, \quad (1)$$

which is roughly four times as large as

$$\tau(\Omega_c^0) = 69 \pm 12 \text{ fs} \quad (2)$$

in the Particle Data Group 2018 archive (PDG2018) [2]. In 2021, LHCb confirmed the previous measurement using Ω_c^0 produced directly from proton–proton collision [3], and in 2022, Belle II reported a similar result using $\Omega_c^0 \rightarrow \Omega^- \pi^+$ decays [4]. These recent measurements indicate that Ω_c^0 is not the shortest-lived weakly decaying charmed baryon, which conflicts with our previous understanding [5]. This demands theoretical explanation.

At present, the standard framework for understanding weakly decaying heavy flavor hadrons is heavy quark expansion (HQE) [6–13]. Under this framework, some attempts have been made to resolve the Ω_c lifetime puzzle [14–16].

However, there is still a lack of more reliable calculation based on quantum chromodynamics (QCD) for the hadronic matrix elements of high-dimensional operators in HQE.

HQE describes inclusive weak decays of heavy flavor hadrons. It is a generalization of the operator product expansion (OPE) in $1/m_Q$, and enables the systematic study of non-perturbative effects. The starting point of HQE is the following transition operator

$$\mathcal{T} = i \int d^4x T[\mathcal{L}_W(x)\mathcal{L}_W^\dagger(0)], \quad (3)$$

where \mathcal{L}_W is the effective weak Lagrangian governing the decay $Q \rightarrow X_f$. The total decay width of a hadron H_Q containing a heavy quark Q can be given as

$$\Gamma(H_Q) = \frac{2 \text{Im}\langle H_Q | \mathcal{T} | H_Q \rangle}{2M_H}, \quad (4)$$

where M_H is the mass of H_Q . The right-hand side of Eq. (4) is then calculated using OPE for the transition operator \mathcal{T} [5, 14]

$$2 \text{Im}\mathcal{T} = \frac{G_F^2 m_Q^5}{192\pi^3} \xi \left(c_{3,Q} \bar{Q}Q + \frac{c_{5,Q}}{m_Q^2} \bar{Q}g_s\sigma \cdot GQ + \frac{c_{6,Q}}{m_Q^3} T_6 + \dots \right), \quad (5)$$

where ξ is the relevant Cabibbo–Kobayashi–Maskawa (CKM) matrix element, and T_6 consists of the four-quark operators $(\bar{Q}\Gamma q)(\bar{q}\Gamma Q)$, with Γ representing a combination of Dirac and color matrices.

In fact, there was also a conflict between theory and experiment for the lifetime of Λ_b as early as 1996. Taking $\tau(B^0) = (1.519 \pm 0.004) \text{ ps}$ in PDG2022 [17] as a benchmark, for $\tau(\Lambda_b) = (1.14 \pm 0.08) \text{ ps}$ in PDG1996 [18], one can find the ratio

$$\tau(\Lambda_b^0)/\tau(B^0) = 0.75 \pm 0.05. \quad (6)$$

^a e-mail: zhaozx19@imu.edu.cn (corresponding author)

^b e-mail: zpxing@sjtu.edu.cn

Theoretically, the ratio deviating from unity at the level of 20% is considered to be too large. Nowadays, we know that the low value of $\tau(\Lambda_b)/\tau(B_d)$ or the short Λ_b lifetime was a purely experimental issue. The world averages in PDG2022 are

$$\begin{aligned} \tau(\Lambda_b) &= (1.471 \pm 0.009) \text{ ps}, \\ \tau(\Lambda_b^0)/\tau(B^0) &= 0.964 \pm 0.007, \end{aligned} \tag{7}$$

which are in good agreement with the HQE prediction [5]:

$$\begin{aligned} \frac{\tau(\Lambda_b)}{\tau(B_d)} \text{HQE2014} &= 1 - (0.8 \pm 0.5)\%_{1/m_b^2} - (4.2 \pm 3.3)\%_{1/m_b^3} \\ &\quad - (0.0 \pm 0.5)\%_{1/m_b^3}^{B_d} - (1.6 \pm 1.2)\%_{1/m_b^4} \\ &= 0.935 \pm 0.054. \end{aligned} \tag{8}$$

However, it can be seen from Eq. (8) that the main uncertainty in the lifetime ratio comes from the $1/m_b^3$ corrections of the Λ_b -matrix elements. The relevant matrix elements can be parameterized in a model-independent way as follows [14]:

$$\begin{aligned} \langle \Lambda_b | (\bar{b}q)_{V-A} (\bar{q}b)_{V-A} | \Lambda_b \rangle &= f_{B_q}^2 m_{B_q} m_{\Lambda_b} L_1, \\ \langle \Lambda_b | (\bar{b}q)_{S-P} (\bar{q}b)_{S+P} | \Lambda_b \rangle &= f_{B_q}^2 m_{B_q} m_{\Lambda_b} L_2, \\ \langle \Lambda_b | (\bar{b}^\alpha q^\beta)_{V-A} (\bar{q}^\beta b^\alpha)_{V-A} | \Lambda_b \rangle &= f_{B_q}^2 m_{B_q} m_{\Lambda_b} L_3, \\ \langle \Lambda_b | (\bar{b}^\alpha q^\beta)_{S-P} (\bar{q}^\beta b^\alpha)_{S+P} | \Lambda_b \rangle &= f_{B_q}^2 m_{B_q} m_{\Lambda_b} L_4, \end{aligned} \tag{9}$$

where $(\bar{q}_1 q_2)_{V-A} \equiv \bar{q}_1 \gamma_\mu (1 - \gamma_5) q_2$ and $(\bar{q}_1 q_2)_{S\pm P} \equiv \bar{q}_1 (1 \pm \gamma_5) q_2$. In the literature, a \tilde{B} is usually introduced to relate L_3 to L_1

$$L_3 = -\tilde{B} L_1. \tag{10}$$

The theoretical predictions for L_1 , L_2 and \tilde{B} are listed in Table 1, from which one can see that there are significant differences in the theoretical predictions for L_1 and L_2 . In this work, we intend to clarify this issue.

In Ref. [24], we performed a QCD sum rules analysis of the weak decay form factors of doubly heavy baryons to singly heavy baryons. However, considering that there were few theoretical predictions and experimental data available to compare with, we then applied our calculation method to study the semileptonic decay of $\Lambda_b \rightarrow \Lambda_c l \bar{\nu}$ in Ref. [25]. It turned out that our predictions for the form factors and decay widths were consistent with those of heavy quark effective theory (HQET) and lattice QCD. In this work, similar computing strategies are undertaken. At the QCD level, contributions from up to dimension-6 four-quark operators are considered to obtain the matrix elements in Eq. (9).

The remainder of this article is organized as follows. In Sect. 2, the main steps of QCD sum rules are presented, and in Sect. 3, numerical results are shown. For consistency, the pole residue of Λ_b is also considered. We conclude this article in the last section.

2 QCD sum rules analysis

The following interpolating current is adopted for Λ_b :

$$J = \epsilon_{abc} (u_a^T C \gamma_5 d_b) Q_c, \tag{11}$$

where Q denotes the bottom quark, a, b, c are color indices, and C is the charge conjugation matrix. The correlation function is defined as

$$\Pi(p_1, p_2) = i^2 \int d^4x d^4y e^{-ip_1 \cdot x + ip_2 \cdot y} \langle 0 | T \{ J(y) \Gamma_6(0) \bar{J}(x) \} | 0 \rangle, \tag{12}$$

with Γ_6 being a four-quark operator given in Eq. (9). Note that in spin space, $J(y)$, $\Gamma_6(0)$ and $\bar{J}(x)$ are 4×1 , 1×1 , and 1×4 matrices, respectively, and therefore $\Pi(p_1, p_2)$ is a 4×4 matrix.

Following the standard procedure of QCD sum rules, one can calculate the correlation function at the hadron and QCD levels. At the hadron level, after inserting the complete set of baryon states, one can obtain

$$\Pi^{\text{had}}(p_1, p_2) = \lambda_H^2 \frac{(\not{p}_2 + M)(a + b\gamma_5)(\not{p}_1 + M)}{(p_2^2 - M^2)(p_1^2 - M^2)} + \dots, \tag{13}$$

where $\lambda_H = \lambda_{\Lambda_b}$, $M = m_{\Lambda_b}$ are respectively the pole residue and mass of Λ_b , the parameters a and b are introduced to parameterize the hadronic matrix element

$$\langle \Lambda_b(q', s') | \Gamma_6 | \Lambda_b(q, s) \rangle = \bar{u}(q', s')(a + b\gamma_5)u(q, s), \tag{14}$$

and the ellipsis stands for the contribution from higher excited states. For the forward scattering matrix element, one can show that

$$\begin{aligned} \langle \Lambda_b(q, s) | \Gamma_6 | \Lambda_b(q, s) \rangle &= \bar{u}(q, s)(a + b\gamma_5)u(q, s) \\ &= 2 a m_{\Lambda_b}, \end{aligned} \tag{15}$$

where $\bar{u}(q, s)u(q, s) = 2 m_{\Lambda_b}$ and $\bar{u}(q, s)\gamma_5 u(q, s) = 0$ have been used. One can see that only the parameter a in Eq. (14) is relevant to the forward scattering matrix element.

It can be seen from Eq. (13) that there are eight Dirac structures, but only (at most) two parameters need to be determined. By considering the contribution of negative-parity baryons [24–26], one can update Eq. (13) to

$$\begin{aligned} \Pi^{\text{had}}(p_1, p_2) &= \lambda_+ \lambda_+ \frac{(\not{p}_2 + M_+)(a^{++} + b^{++}\gamma_5)(\not{p}_1 + M_+)}{(p_2^2 - M_+^2)(p_1^2 - M_+^2)} \\ &\quad + \lambda_+ \lambda_- \frac{(\not{p}_2 + M_+)(a^{+-} + b^{+-}\gamma_5)(\not{p}_1 - M_-)}{(p_2^2 - M_+^2)(p_1^2 - M_-^2)} \\ &\quad + \lambda_- \lambda_+ \frac{(\not{p}_2 - M_-)(a^{-+} + b^{-+}\gamma_5)(\not{p}_1 + M_+)}{(p_2^2 - M_-^2)(p_1^2 - M_+^2)} \\ &\quad + \lambda_- \lambda_- \frac{(\not{p}_2 - M_-)(a^{--} + b^{--}\gamma_5)(\not{p}_1 - M_-)}{(p_2^2 - M_-^2)(p_1^2 - M_-^2)} \\ &\quad + \dots \end{aligned} \tag{16}$$

Table 1 L_1, L_2 and \tilde{B} predicted by different theoretical methods. This table is reproduced from Ref. [5]

L_1	L_2	\tilde{B}	
-0.103(10)	0.069(7)	1	2014 Spectroscopy update [19]
-0.22(4)	0.17(2)	1.21(34)	1999 Exploratory Lattice [20]
-0.22(5)	0.14(3)	1	1999 QCDSR v1 [21]
-0.60(15)	0.40(10)	1	1999 QCDSR v2 [21]
-0.033(17)	0.022(11)	1	1996 QCDSR [22]
≈ -0.03	≈ 0.02	1	1979 Bag model [23]
≈ -0.08	≈ 0.06	1	1979 NRQM [23]

Here, $M_{+(-)}$ and $\lambda_{+(-)}$ respectively denote the mass and pole residue of $\Lambda_b(1/2^{+(-)})$, and a^{+-} is the parameter a for the positive-parity final state $\Lambda_b(1/2^+)$ and the negative-parity initial state $\Lambda_b(1/2^-)$, and so forth. When arriving at Eq. (16), we have adopted the following conventions:

$$\begin{aligned}
 &\langle \Lambda_{b+}(q', s') | \Gamma_6 | \Lambda_{b+}(q, s) \rangle \\
 &= \bar{u}_+(q', s')(a^{++} + b^{++} \gamma_5) u_+(q, s), \\
 &\langle \Lambda_{b+}(q', s') | \Gamma_6 | \Lambda_{b-}(q, s) \rangle \\
 &= \bar{u}_+(q', s')(a^{+-} + b^{+-} \gamma_5) (i \gamma_5) u_-(q, s), \\
 &\langle \Lambda_{b-}(q', s') | \Gamma_6 | \Lambda_{b+}(q, s) \rangle \\
 &= \bar{u}_-(q', s')(i \gamma_5) (a^{-+} + b^{-+} \gamma_5) u_+(q, s), \\
 &\langle \Lambda_{b-}(q', s') | \Gamma_6 | \Lambda_{b-}(q, s) \rangle \\
 &= \bar{u}_-(q', s')(i \gamma_5) (a^{--} + b^{--} \gamma_5) (i \gamma_5) u_-(q, s). \quad (17)
 \end{aligned}$$

In Eq. (17), these $i \gamma_5$ are not necessary, but they are convenient.

At the QCD level, the correlation function can be written formally as

$$\begin{aligned}
 \Pi^{\text{QCD}}(p_1, p_2) = & A_1 \not{p}_2 \not{p}_1 + A_2 \not{p}_2 + A_3 \not{p}_1 + A_4 \\
 & + A_5 \not{p}_2 \gamma_5 \not{p}_1 + A_6 \not{p}_2 \gamma_5 \\
 & + A_7 \gamma_5 \not{p}_1 + A_8 \gamma_5. \quad (18)
 \end{aligned}$$

The coefficients A_i are then expressed as double dispersion relations

$$A_i(p_1^2, p_2^2, q^2) = \int_0^\infty ds_1 \int_0^\infty ds_2 \frac{\rho^{A_i}(s_1, s_2, q^2)}{(s_1 - p_1^2)(s_2 - p_2^2)}, \quad (19)$$

where the spectral function $\rho^{A_i}(s_1, s_2, q^2)$ can be calculated using Cutkosky cutting rules, see Fig. 1. Sum rules are obtained by equating Eq. (16) with Eq. (18) and then using quark-hadron duality to eliminate the contribution of excited states. Furthermore, by equating the coefficients of the same Dirac structure, one can have eight $\pm\pm$ equations to solve eight unknown parameters $a^{\pm\pm}$ and $b^{\pm\pm}$. In particular, after per-

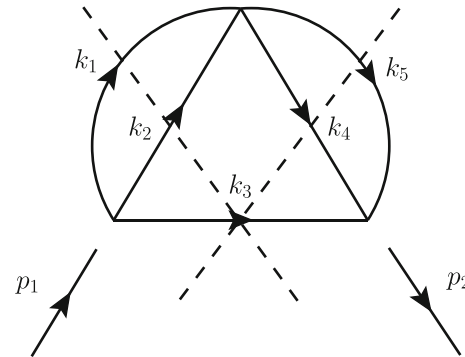


Fig. 1 Perturbative contribution. Cutting rules are also shown

forming the Borel transform, one can arrive at

$$\begin{aligned}
 a^{++} = & \frac{\{M_-^2, M_-, M_-, 1\} \cdot \{\mathcal{B}A_1, \mathcal{B}A_2, \mathcal{B}A_3, \mathcal{B}A_4\}}{\lambda_+^2 (M_+ + M_-)^2} \\
 & \exp\left(\frac{2M_+^2}{T^2}\right), \quad (20)
 \end{aligned}$$

where $\mathcal{B}A_i$ are doubly Borel-transformed coefficients

$$\mathcal{B}A_i = \int_0^{s_0} ds_1 \int_0^{s_0} ds_2 \rho^{A_i}(s_1, s_2, q^2) \exp\left(-\frac{s_1 + s_2}{T^2}\right), \quad (21)$$

and s_0 and T^2 are the continuum threshold parameter and the Borel parameter, respectively.

In this work, contributions from up to dimension-6 four-quark operators are considered at the QCD level.¹ For the matrix elements in Eq. (9), we find that contributions from quark condensate (dimension-3) and quark-gluon condensate (dimension-5) are proportional to the mass of the u/d quark, which is taken to be zero in this work. All nonzero, “independent” diagrams are shown in Fig. 2. Here, “independent” implies non-equivalence. For example, diagram dim-4-2,5 with quark 2 and quark 5 each emitting a gluon is equal to diagram dim-4-1,4; therefore, the former is not listed in Fig. 2.

¹ Readers should not confuse the four-quark operators in HQE with those at the QCD level in QCD sum rules.

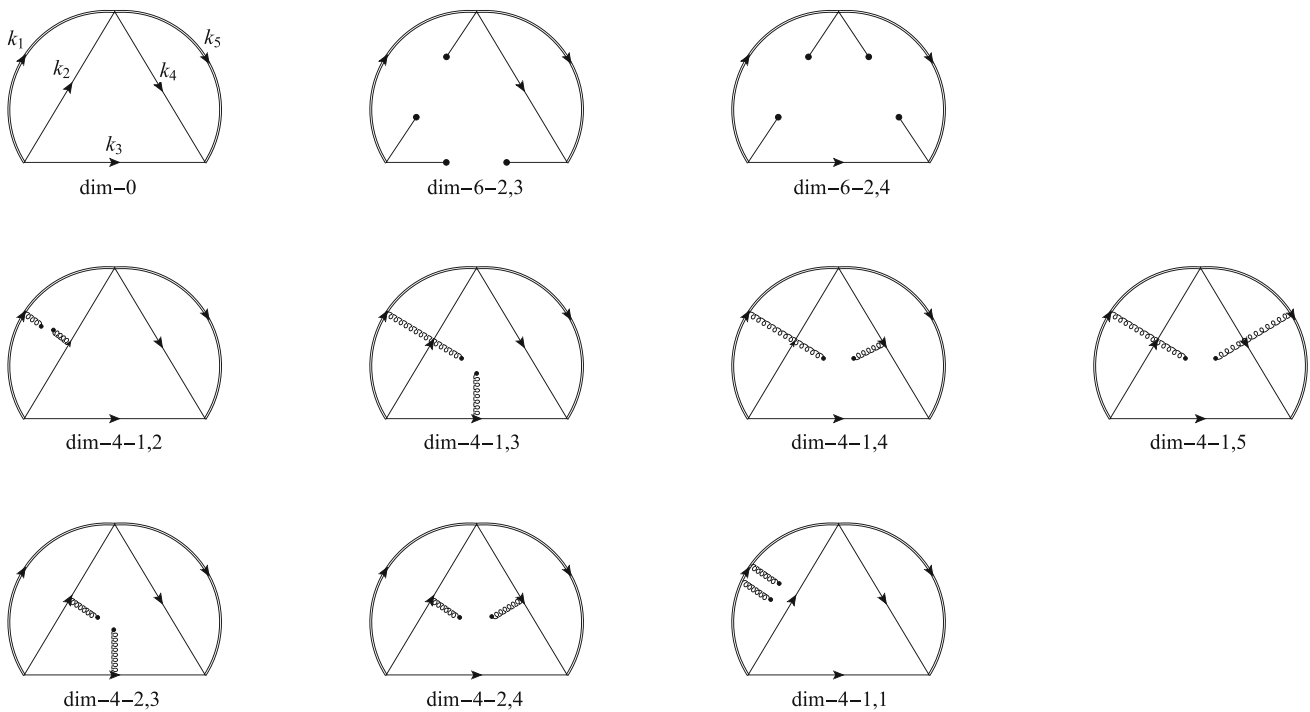


Fig. 2 All nonzero, “independent” diagrams considered in this work

2.1 The pole residue

As can be seen in Eq. (20), the pole residue of Λ_b is an indispensable input. For consistency, in this work, we also perform an analysis on the pole residue of Λ_b , whose sum rule is [25]

$$\begin{aligned} & (M_+ + M_-)\lambda_+^2 \exp(-M_+^2/T_+^2) \\ &= \int^{s_0} ds (M_- \rho^A + \rho^B) \exp(-s/T_+^2), \end{aligned} \tag{22}$$

from which, one can obtain the mass formula for Λ_b

$$M_+^2 = \frac{\int^{s_0} ds (M_- \rho^A + \rho^B) s \exp(-s/T_+^2)}{\int^{s_0} ds (M_- \rho^A + \rho^B) \exp(-s/T_+^2)}. \tag{23}$$

Equation (23) can be viewed as a constraint to Eq. (22). Following Ref. [27], in this work, we use Eq. (23) to determine the continuum threshold parameter s_0 . Specifically, for a set of fixed parameters (renormalization scale, condensate parameters, etc.), the optimal (s_0, T_+^2) are obtained through the following procedure:

1. For a trial s_0 , plot the pole residue curve with respect to the Borel parameter T_+^2 using Eq. (22). Find the minimum point T_+^2 on the curve (see Fig. 3 for some intuitive impressions).
2. Substitute the set of (s_0, T_+^2) obtained in step 1 into Eq. (23) to calculate the baryon mass, and compare it with the

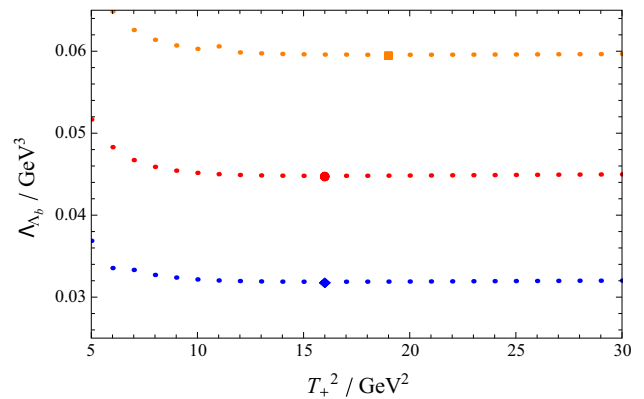


Fig. 3 The pole residue λ_{Λ_b} as a function of the Borel parameter T_+^2 . The red, orange and blue dots respectively correspond to the renormalization scales $\mu = m_b$, $\mu = 6$ GeV and $\mu = 3$ GeV. The minimum points are marked, and they correspond to the experimental mass of Λ_b via Eq. (23)

experimental value. If equal (within a small error range), terminate; otherwise, go to step 1.

For different input parameters, one can obtain different optimal (s_0, T_+^2) , which are listed in Table 2.

In this work, contributions from up to dimension-6 four-quark operators are also considered for the sum rule in Eq. (22).

3 Numerical results

3.1 Inputs

Our main inputs in numerical calculation can be found in Table 2. We take the $\overline{\text{MS}}$ mass for the bottom quark [17] and neglect the mass of the u/d quark. The condensate parameters are taken from Ref. [28]. The renormalization scale is taken as $\mu_b = 3\text{--}6$ GeV, with $m_b(m_b)$ the central value [27], from which one can estimate the dependence of the calculation results on the renormalization scale.

3.2 The pole residue and the continuum threshold parameter

Our predictions for the pole residue λ_{Λ_b} , together with the continuum threshold parameter s_0 , can be found in Table 2. A similar investigation was also performed in our previous work [25]; however, in this work, more contributions from higher-dimensional operators are considered. Numerically, the predictions in this work are close to those in Ref. [25]. This is essentially because the contributions from higher-dimensional operators are small. A comprehensive study of the pole residues of anti-triplet heavy baryons can be found in Ref. [29].

3.3 The four-quark operator matrix elements

The four-quark operator matrix elements in Eq. (9) are all proportional to some parameter L_i . In Fig. 4, we plot the curves of $L_{1,2,3,4}$ as functions of the Borel parameter T^2 , on which the stability region can be found. In these figures, we have also evaluated the dependence of $L_{1,2,3,4}$ on the renormalization scale. The corresponding results are summarized in Table 2.

Adding all the uncertainties from various input parameters in quadrature, our final results of $L_{1,2,3,4}$ and $\tilde{B} \equiv -L_3/L_1$ are respectively

$$\begin{aligned} L_1 &= -0.143 \pm 0.028, \\ L_2 &= +0.0746 \pm 0.0142, \\ L_3 &= +0.151 \pm 0.027, \\ L_4 &= -0.0764 \pm 0.0139, \end{aligned} \quad (24)$$

and

$$\tilde{B} = 1.057 \pm 0.030, \quad (25)$$

where $m_{B_q} = 5.280$ GeV and $f_{B_q} = 186$ MeV [14] have been used.

Some comments are in order.

- The spectral density in Eq. (19) also depends on $q^2 \equiv (p_1 - p_2)^2$. For the forward scattering matrix elements of interest, q^2 is taken to be 0.
- In Eq. (9), the only difference between the first matrix element $\langle \Lambda_b | (\bar{b}q)_{V-A} (\bar{q}b)_{V-A} | \Lambda_b \rangle$ and the third matrix element $\langle \Lambda_b | (\bar{b}^\alpha q^\beta)_{V-A} (\bar{q}^\beta b^\alpha)_{V-A} | \Lambda_b \rangle$ is in the color space. For all the diagrams in Fig. 2 except for diagrams (dim-4-1,4), (dim-4-1,5) and (dim-4-2,4), the color factors for the two matrix elements differ only by a negative sign. Considering that the contributions of these three gluon condensate diagrams are small, $\tilde{B} \equiv -L_3/L_1$ only deviates slightly by 1.
- One can see from Table 2 that the uncertainty caused by μ dependence is dominant, which is about 20%. As a comparison, in Ref. [27], the authors performed a QCD sum rules analysis on the decay constants of B and B_s mesons. μ is also taken in the range of 3–6 GeV with $m_b(m_b)$ as the central value. For the perturbative spectral function, contributions from up to α_s^2 order are considered. Scale dependence is also the main source of error, which is approximately 10%. It can be expected that when higher-order corrections are considered, the scale dependence should decrease.
- In Fig. 4, we have also shown the calculation errors, which are essentially small. Nevertheless, when we try to find the stability region on the curve, these small errors also play a role.
- As can be seen in Table 2, for a set of fixed parameters (quark mass, renormalization scale, condensate parameters), the continuum threshold parameter s_0 can be determined, and then the quantities we are interested in can also be determined—by requiring them to have as little dependence on the Borel parameter as possible.
- In our opinion, the continuum threshold parameter s_0 is the most important parameter in QCD sum rules. In fact, once s_0 is fixed, the quantity that we are interested in is almost determined by searching for the stability region. In the literature, there exist at least two approaches for determining s_0 . One approach is to empirically select $\sqrt{s_0}$ approximately 0.5 GeV larger than the ground state mass. Another approach is to determine s_0 through the mass formula. We have adopted the latter approach in this work. The basic logic behind doing so is that the mass formula can be seen as a constraint to the sum rule of the two-point correlation function. Of course, this comes with the cost of abandoning the predictive power of hadron mass.

4 Conclusions

Heavy quark expansion can nicely explain the lifetime of Λ_b . However, there still exist sizable uncertainties in the four-quark operator matrix elements of Λ_b in $1/m_b^3$ corrections,

Fig. 4 $L_{1,2,3,4}$ as functions of the Borel parameter T^2

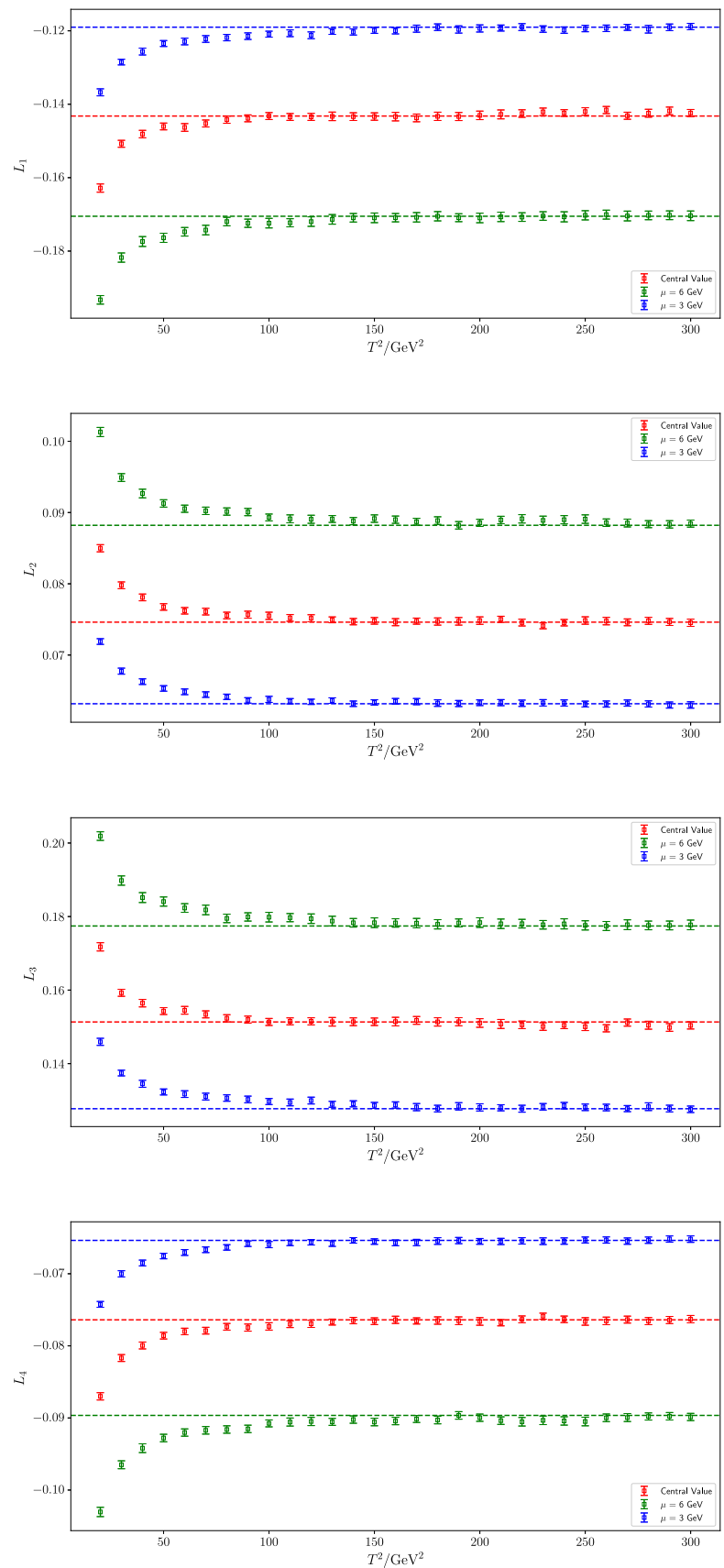


Table 2 Our predictions of the pole residue λ_{Λ_b} , $L_{1,2,3,4}$ defined in Eq. (9), and $\tilde{B} \equiv -L_3/L_1$. For a set of fixed parameters (renormalization scale, condensate parameters, etc.), the continuum threshold parameter

s_0 can be determined, and then the quantities we are interested in can also be determined—by requiring them to have as little dependence on the Borel parameter as possible

	Central value	$m_b/\text{GeV} = 4.18 \pm 0.03$	$\mu/\text{GeV} = 6.0$ $\mu/\text{GeV} = 3.0$	$\langle \bar{q}q \rangle (1 \text{ GeV})/\text{GeV}^3 = -(0.24 \pm 0.01)^3$	$\langle g_s^2 GG \rangle/\text{GeV}^4 = 0.47 \times (1.0 \pm 0.3)$	$m_{\Lambda_b}/\text{GeV} = 5.620 \pm 0.001$
s_0/GeV^2	36.08	36.08 36.01	36.09 36.03	36.09 36.04	36.08 36.08	36.09 36.07
T_+^2/GeV^2	16	16 17	19 16	19 14	16 16	16 16
λ_{Λ_b}	0.0448	0.0429 0.0465	0.0596 0.0319	0.0452 0.0443	0.0448 0.0448	0.0449 0.0447
$\Delta\lambda_{\Lambda_b}$	–	–0.0019 +0.0017	+0.0148 –0.0129	+0.0004 –0.0005	–0.0000 +0.0000	+0.0001 –0.0001
T^2/GeV^2	100	150 180	180 180	150 120	100 90	150 120
L_1	–0.143	–0.139 –0.144	–0.171 –0.119	–0.150 –0.136	–0.144 –0.143	–0.143 –0.143
ΔL_1	–	+0.004 –0.001	–0.027 +0.024	–0.007 +0.007	–0.001 +0.001	–0.000 +0.000
T^2/GeV^2	100	210 240	260 220	270 120	100 90	150 120
L_3	0.151	0.147 0.151	0.177 0.128	0.156 0.144	0.154 0.148	0.151 0.151
ΔL_3	–	–0.004 –0.000	+0.026 –0.024	+0.005 –0.007	+0.003 –0.003	–0.000 –0.000
$\tilde{B} = -L_3/L_1$	1.057	1.056 1.049	1.041 1.073	1.040 1.060	1.073 1.040	1.056 1.056
$\Delta\tilde{B}$	–	–0.000 –0.007	–0.016 +0.017	–0.016 +0.003	+0.017 –0.017	–0.001 –0.000
T^2/GeV^2	160	170 200	190 140	220 190	160 160	140 180
L_2	0.0746	0.0728 0.0750	0.0882 0.0632	0.0780 0.0713	0.0758 0.0733	0.0745 0.0744
ΔL_2	–	–0.0018 +0.0004	+0.0136 –0.0114	+0.0033 –0.0033	+0.0011 –0.0013	–0.0001 –0.0002
T^2/GeV^2	160	170 200	190 140	220 190	160 160	140 180
L_4	–0.0764	–0.0746 –0.0767	–0.0896 –0.0654	–0.0797 –0.0732	–0.0781 –0.0745	–0.0763 –0.0762
ΔL_4	–	+0.0018 –0.0003	–0.0133 +0.0110	–0.0033 +0.0032	–0.0017 +0.0018	+0.0001 +0.0002

which describe the spectator effects. In this work, these four-quark operator matrix elements are investigated using full QCD sum rules. At the QCD level, contributions from up to dimension-6 four-quark operators are considered. A stable Borel region can be found. We have also considered the uncertainties from various input parameters, and find that the main source of error is scale dependence, which is about 20%. Our method for calculating high-dimensional operator matrix elements holds promise for use in resolving the Ω_c lifetime puzzle.

Acknowledgements The authors are grateful to Profs. Pietro Colangelo, Yue-Long Shen, Wei Wang, Zhi-Gang Wang, Fu-Sheng Yu, and Dr. Yu-Ji Shi for valuable discussions. This work is supported in part by scientific research start-up fund for Junma program of Inner Mongolia University, scientific research start-up fund for talent introduction in Inner Mongolia Autonomous Region, and National Natural Science Foundation of China under Grant No. 12065020.

Data Availability Statement This manuscript has no associated data or the data will not be deposited. [Authors’ comment: If readers are interested in more calculation details, they can contact the authors].

Open Access This article is licensed under a Creative Commons Attribution 4.0 International License, which permits use, sharing, adaptation, distribution and reproduction in any medium or format, as long as you

give appropriate credit to the original author(s) and the source, provide a link to the Creative Commons licence, and indicate if changes were made. The images or other third party material in this article are included in the article's Creative Commons licence, unless indicated otherwise in a credit line to the material. If material is not included in the article's Creative Commons licence and your intended use is not permitted by statutory regulation or exceeds the permitted use, you will need to obtain permission directly from the copyright holder. To view a copy of this licence, visit <http://creativecommons.org/licenses/by/4.0/>.
Funded by SCOAP³.

References

1. R. Aaij et al. [LHCb], Phys. Rev. Lett. **121**(9), 092003 (2018). <https://doi.org/10.1103/PhysRevLett.121.092003>. arXiv:1807.02024 [hep-ex]
2. M. Tanabashi et al. [Particle Data Group], Phys. Rev. D **98**(3), 030001 (2018). <https://doi.org/10.1103/PhysRevD.98.030001>
3. R. Aaij et al. [LHCb], Sci. Bull. **67**(5), 479–487 (2022). <https://doi.org/10.1016/j.scib.2021.11.022>. arXiv:2109.01334 [hep-ex]
4. F.J. Abudinen et al. [Belle-II], Phys. Rev. D **107**(3), L031103 (2023). <https://doi.org/10.1103/PhysRevD.107.L031103>. arXiv:2208.08573 [hep-ex]
5. A. Lenz, Int. J. Mod. Phys. A **30**(10), 1543005 (2015). <https://doi.org/10.1142/S0217751X15430058>. arXiv:1405.3601 [hep-ph]
6. V.A. Khoze, M.A. Shifman, Sov. Phys. Usp. **26**, 387 (1983). <https://doi.org/10.1070/PU1983v026n05ABEH004398>
7. I.I.Y. Bigi, N.G. Uraltsev, Phys. Lett. B **280**, 271–280 (1992). [https://doi.org/10.1016/0370-2693\(92\)90066-D](https://doi.org/10.1016/0370-2693(92)90066-D)
8. I.I.Y. Bigi, N.G. Uraltsev, A.I. Vainshtein, Phys. Lett. B **293**, 430–436 (1992) [Erratum: Phys. Lett. B **297**, 477–477 (1992)]. [https://doi.org/10.1016/0370-2693\(92\)90908-M](https://doi.org/10.1016/0370-2693(92)90908-M). arXiv:hep-ph/9207214
9. B. Blok, M.A. Shifman, Nucl. Phys. B **399**, 441–458 (1993). [https://doi.org/10.1016/0550-3213\(93\)90504-I](https://doi.org/10.1016/0550-3213(93)90504-I). arXiv:hep-ph/9207236
10. B. Blok, M.A. Shifman, Nucl. Phys. B **399**, 459–476 (1993). [https://doi.org/10.1016/0550-3213\(93\)90505-J](https://doi.org/10.1016/0550-3213(93)90505-J). arXiv:hep-ph/9209289
11. M. Neubert, Adv. Ser. Direct. High Energy Phys. **15**, 239–293 (1998). https://doi.org/10.1142/9789812812667_0003. arXiv:hep-ph/9702375
12. N. Uraltsev, Proc. Int. Sch. Phys. Fermi **137**, 329–409 (1998). <https://doi.org/10.3254/978-1-61499-222-6-329>. arXiv:hep-ph/9804275
13. I.I.Y. Bigi, arXiv:hep-ph/9508408
14. H.Y. Cheng, JHEP **11**, 014 (2018). [https://doi.org/10.1007/JHEP11\(2018\)014](https://doi.org/10.1007/JHEP11(2018)014). arXiv:1807.00916 [hep-ph]
15. J. Gratex, B. Melić, I. Nišandžić, JHEP **07**, 058 (2022). [https://doi.org/10.1007/JHEP07\(2022\)058](https://doi.org/10.1007/JHEP07(2022)058). arXiv:2204.11935 [hep-ph]
16. H.Y. Cheng, C.W. Liu, arXiv:2305.00665 [hep-ph]
17. R.L. Workman et al. [Particle Data Group], PTEP **2022**, 083C01 (2022). <https://doi.org/10.1093/ptep/ptac097>
18. R.M. Barnett et al. [Particle Data Group], Phys. Rev. D **54**(1), 1–720 (1996). <https://doi.org/10.1103/PhysRevD.54.1>
19. J.L. Rosner, Phys. Lett. B **379**, 267–271 (1996). [https://doi.org/10.1016/0370-2693\(96\)00352-8](https://doi.org/10.1016/0370-2693(96)00352-8). arXiv:hep-ph/9602265
20. M. Di Pierro et al. [UKQCD], Phys. Lett. B **468**, 143 (1999) [Erratum: Phys. Lett. B **525**, 360–360 (2002)]. [https://doi.org/10.1016/S0370-2693\(99\)01166-1](https://doi.org/10.1016/S0370-2693(99)01166-1). arXiv:hep-lat/9906031
21. C.S. Huang, C. Liu, S.L. Zhu, Phys. Rev. D **61**, 054004 (2000). <https://doi.org/10.1103/PhysRevD.61.054004>. arXiv:hep-ph/9906300
22. P. Colangelo, F. De Fazio, Phys. Lett. B **387**, 371–378 (1996). [https://doi.org/10.1016/0370-2693\(96\)01049-0](https://doi.org/10.1016/0370-2693(96)01049-0). arXiv:hep-ph/9604425
23. B. Guberina, S. Nussinov, R.D. Peccei, R. Ruckl, Phys. Lett. B **89**, 111–115 (1979). [https://doi.org/10.1016/0370-2693\(79\)90086-8](https://doi.org/10.1016/0370-2693(79)90086-8)
24. Y.J. Shi, W. Wang, Z.X. Zhao, Eur. Phys. J. C **80**(6), 568 (2020). <https://doi.org/10.1140/epjc/s10052-020-8096-2>. arXiv:1902.01092 [hep-ph]
25. Z.X. Zhao, R.H. Li, Y.L. Shen, Y.J. Shi, Y.S. Yang, Eur. Phys. J. C **80**(12), 1181 (2020). <https://doi.org/10.1140/epjc/s10052-020-08767-1>. arXiv:2010.07150 [hep-ph]
26. Z.X. Zhao, R.H. Li, Y.J. Shi, S.H. Zhou, arXiv:2005.05279 [hep-ph]
27. M. Jamin, B.O. Lange, Phys. Rev. D **65**, 056005 (2002). <https://doi.org/10.1103/PhysRevD.65.056005>. arXiv:hep-ph/0108135
28. P. Colangelo, A. Khodjamirian, https://doi.org/10.1142/9789812810458_0033. arXiv:hep-ph/0010175
29. Z.G. Wang, Eur. Phys. J. C **68**, 479–486 (2010). <https://doi.org/10.1140/epjc/s10052-010-1365-8>. arXiv:1001.1652 [hep-ph]